Experimental study of geometry dependence of scalar transfer efficiency of rough surfaces

Aya Hagishima[a], Naoki Ikegaya[b], Yudai Tanaka[c],
Jun Tanimoto[d], Ken-ichi Narita[e]

[a]*Kyushu University, Fukuoka, Japan, ayahagishima@kyudai.jp*
[b]*Kyushu University, Fukuoka, Japan, ikegaya.naoki@kyudai.jp*
[c]*Kyushu University, Fukuoka, Japan, y.tanaka@kyudai.jp*
[d]*Kyushu University, Fukuoka, Japan,tanimoto@cm.kyushu-u.ac.jp*
[e]*Nippon Institute of Technology, Saitama, Japan, narita@nit.ac.jp*

ABSTRACT: The authors performed a series of wind tunnel experiments under neutral conditions to create a comprehensive database of scalar transfer coefficients of street surfaces of regular block arrays; the purpose of creating this database was to improve the wall function of scalar transfer used for computational simulation of an urban environment. We estimated the scalar transfer rate (C_E) using the salinity method. The configuration of the block arrays was designed to be same as those used in a previous experiment on the total drag force acting on arrays. The results for cubical arrays showed that the scalar transfer coefficients for staggered and square layouts produced different tendencies against the roughness packing density. The results also indicated that the effect of layout on C_E was small under the sparse roughness condition, which resulted in isolated flow. In addition, block arrays enhanced the scalar transfer of the street surface under the condition of isolated flow or wake interference flow. In contrast, C_E for dense roughness packing density differed according to the layout of the blocks.

1 INTRODUCTION

Momentum, heat, and scalar transfer processes between an urban rough surface and atmosphere are closely related to the urban atmospheric environment near a ground surface. Hence, understanding how urban geometry affects these phenomena is important from the viewpoints of urban climatology and wind engineering. For example, several aerodynamic parameters describe spatio-temporal averaged features of urban wind, such as roughness length, displacement height, and drag coefficient, and have been investigated intensively for decades in wind tunnel experiments and numerical simulations (Cheng and Castro, 2002; Coceal et al., 2006; Kanda, 2006, Grimmond and Oke, 1999). From the viewpoint of meso-scale modeling, other research has investigated the scalar transfer process between bulk urban surfaces and air; also, a relation between the sublayer Stanton number for rough surfaces and the roughness Reynolds number Re_* has been suggested (Brutsaert, 1982; Chamberblain, 1968; Owen and Thomson, 1963) based on experimental and theoretical approaches. Kanda and Moriizumi (2009) recently clarified that a relation of roughness length of momentum and heat against Re_* universally exists among different length scales, from wind tunnel scale to actual urban scale.

However, the universal estimation of scalar transfer efficiency between each component of urban surfaces (such as a roofs, walls, and streets) and air still remains to be discussed.

This has become an important subject because computational simulation of urban atmospheric environments is widely used for both practical assessment and academic research.

It is known that the momentum transfer between a fully rough surface and air is mainly dominated by pressure drag, and not by friction drag; therefore, the Reynolds number dependence of the drag coefficient tends to be negligible. In contrast, there is no corresponding mechanism of pressure drag for the scalar transfer between a surface and air. Within a thin sublayer near a surface, only molecular diffusion dominates the scalar transfer process. Therefore, the ambiguity of the wall function inevitably affects the accuracy of a numerical simulation of the scalar transfer process.

Several measurements of scalar transfer speed of urban-like canopy surfaces have been conducted in not only urban climatology, but also in other mechanical engineering fields. Chyu and Goldstein (1986) measured the mass transfer coefficient of a 2-D cavity using the naphthalene sublimation method. Barlow et al. (2004) investigated the transfer coefficient of the surfaces of 2-D canopies with different aspect ratios using the naphthalene sublimation method, and they discussed the effect of the source area situation. Pascheke et al. (2008) also performed an experiment using the naphthalene sublimation technique to estimate the scalar transfer coefficient of a cubical array and an array with non-uniform height under a condition of a plan area index (hereafter λ_p) of 25%, and investigated the effect of height variability of roughness. Narita (2007) presented the transfer coefficient for surfaces of both 2-D and 3-D canopies based on the wet-filter paper method. Hagishima et al. (2005) made an intercomparison of the transfer coefficient of heat and mass based on previous wind tunnel experiments and outdoor field observations of building surfaces.

In spite of this previous work, for further understanding the scalar transfer process on an urban surface, the following aspects need to be investigated from the computational fluid dynamics (CFD) view point. First, there are insufficient experimental data that can be used to validate and improve the modeling of scalar transfer. More experiments involving the scalar transfer speed from an urban-like rough surface as well as the velocity field are essential. A variety of roughness configurations is important to improve the modeling, which can elucidate the geometry dependence of scalar transfer.

Therefore, we performed a series of wind tunnel experiments under neutral conditions to create a comprehensive database of scalar transfer rates in various types of regular block arrays. The geometry of the arrays used for measurement was designed to capture the effects of the layout, the aspect ratio of the blocks, and the height variability under different conditions of roughness packing density. In this paper we present the details of the so-called salinity methodology for estimating the amount of scalar transfer from the floor of a block array. In addition, we present the results for cubical arrays with different layouts under different conditions of roughness packing density. The configuration of arrays, length of fetch, and size of scalar source that we used to measure the transfer speed were designed to be approximately the same as those of Hagishima et al. (2009). That study measured the total drag force acting on the arrays and reported the geometry dependence of drag coefficient, roughness length, and displacement height. Thus, we combine our present data on scalar transfer rates and the previous data of Hagishima et al. (2009) to effectively validate and improve CFD modeling of scalar transfer from urban surfaces.

2 EXPERIMENTAL DETAILS

2.1 *Measurement principle of the salinity method*

We estimated the scalar transfer rate using the salinity method. In this method, salt water is the scalar source for measurement, and the amount of evaporation from the salt water surface per unit of time is calculated based on the measured increase of salinity for a fixed period of time under a constant flow condition. The relation between salinity and water mass can be expressed by Equation 1:

$$W_{Water} = \frac{1-c}{c} W_{Sod} \tag{1}$$

where c is salinity of the salt water (kg kg^{-1}), and W_{Sod} and W_{Water} are the mass of sodium chloride and water (kg), respectively. The water mass of salt water can be also defined by the volume V (m^3) and density of water ρ_{water} (kg m^{-3}) as follows:

$$W_{Water} = \rho_{water} V \tag{2}$$

Hence, the mass of sodium chloride can be defined as:

$$W_{Sod} = \left(\frac{c}{1-c}\right) \rho_{water} V \tag{3}$$

If the salinity of salt water changes during a period Δt (s) from time t_b to time t_a, the amount of evaporation per unit of surface area and per unit of time E (kg m^{-2} s^{-1}) can be expressed by Equation 4:

$$E = \frac{\rho_{water} V_a}{A \Delta t} \left(\frac{1-c_b}{c_b} \frac{c_a}{1-c_a} - 1 \right) \tag{4}$$

where A is the area of salt water surface (m^2); subscripts a and b refer to the values for time t_a and t_b. In the following sections we discuss the geometry dependence of the dimensionless transfer coefficient (hereafter, C_E), defined by Equation 5:

$$C_E = \frac{E}{\rho_{air} U_{ref} \left(q_{surf} - q_{ref} \right)} \tag{5}$$

where q_{surf} and q_{ref} refer to the vapor concentration of the salt water surface and air at a reference height (kg m^{-3}), respectively. ρ_{air} is density of air (kg m^{-3}) and U_{ref} is the wind speed at a reference height (m s^{-1}).

2.2 *Configuration of the arrays*

The rough surfaces used for the measurement were regular arrays of rectangular blocks. All blocks had a uniform base of 25 mm × 25 mm; hereafter, L = 25 mm is the basic length scale. The arrays are schematically shown in Figure 1. We investigated two regular cubical arrays: one was a lattice-type square pattern (hereafter referred to as SQ1) and the other was a staggered pattern (hereafter referred to as ST1). The numeral 1 refers to the height of the blocks, that is, 1L.

We measured the evaporation flux from the floor of SQ1 under three conditions of plan area density (the ratio of plan area of the blocks to the area of the total plan area, hereafter

λ_p): 7.7, 17.4, and 30.9%. Four λ_p conditions (7.7, 12.1, 17.4, and 30.9%) were adopted for the ST1 array. The configurations of these arrays were the same as those investigated by Hagishima et al. (2009).

2.3 *Instrumentation*

Figure 2 illustrates the wind tunnel device we used for the measurements. It was an open-circuit wind tunnel with a test section of height 0.9 m, width 0.9 m, and length 4.8 m, and was located in a room. The air temperature of the room was controlled by air-conditioning to remain constant during measurement. Four propeller fans with a propeller diameter of 350 mm and maximum rotational frequency of 1550 rpm were attached at the one end of the tunnel, and we set up a wire mesh in a section at a leeward position approximately 1 m from the fans, to unify the cross-sectional airflow distribution.

We embedded a water tank with base dimensions of 720 mm × 720 mm ($28.8L \times 28.8L$) and depth of 50 mm in a square void in the floor of the wind tunnel at a leeward point approximately 3 m from the wire mesh. The levels of both the water surface and the surrounding floor of the wind tunnel were carefully arranged to be consistent. The floor surrounding the water tank was covered with a rectangular array made of wood, which was the target array for the research. We submerged a rectangular array, the height of which was taller than that of the surrounding array, to keep the same "roof" level, as shown in Figure 2. For the lowest λ_p condition (7.7%), 64 blocks were arranged in the tank. In other words, the whole floor of the test section of the wind tunnel was covered with an identical regular array, and a square-shaped scalar source was installed in the leeward side of the floor with a fetch length for momentum of $120L$. The size of the fetch area and the scalar source were the same as those for the surface drag measurements by Hagishima et al. (2009).

Salinity of the salt water was measured with a salinometer (Guildline Instruments, Autosal 8400B) that had a measurement resolution better than 2×10^{-6} kg/kg. It was calibrated every day using IAPSO (International Association for the Physical Sciences of the Ocean) standard seawater.

Mean wind speed was measured using a Pitot-static tube connected to a differential pressure gauge (Sibata Scientific Technology, ISP-3-20DS). The Pitot-static tube was positioned 500 mm ($20L$) above the leeward edge of the water tank. According to the results of Hagishima et al. (2009), the boundary layer thickness for momentum was assumed to be within $6L$ to $8L$; hence, the height of $20L$ was beyond the boundary layer.

The dew point temperature of the air was measured at the leeward side of the wind tunnel with a cooled mirror dew-point hygrometer (Shinyei, DewStar S-1) with accuracy of $\pm0.2^{\circ}$C. In addition, we measured the temperature of the salt water surface with two thermistor thermometers (TechnolSeven, DS101) with accuracy of $\pm0.1^{\circ}$C, and adopted the averaged value for analysis. The sensors were fixed so as to float on the water surface and be covered with a water screen due to the surface tension of water. We had previously observed the surface temperature distribution of the salt water using an infrared camera (NEC-Sanei, TVS-600) under the condition of wind speed of about 2 m s^{-1}, and confirmed the uniform surface temperature distribution. The air temperature at a height of $20L$ was also measured using one of the thermistor thermometers. The output signals from all of the instruments except the salinometer were recorded every 30 s using a data logger.

The measurement procedure was as follows. First, we made the salt water with an NaCl concentration of around 0.03 kg/kg (3%), which consisted of purified water and NaCl with purity >99.5%. We filled bottles with some of this solution for measurement of salinity and then filled the water tank with the residual water. Next, we circulated air with the wind tun-

nel fans at a wind speed about 2 m s^{-1} for about 2 h, after which we collected four salt water samples and measured the salinity (For all salinity measurements, 500-ml volumetric bottles previously rinsed three times with sample water were used). We measured the salinity of each sample bottle five times, continuously, and calculated the mean salinity of all measured values.

We estimated the evaporation flux E based on Equation 4 and calculated the dimensionless transfer coefficient C_E using Equation 5. We estimated q_{surf} as the saturated vapor concentration of the measured temperature of the water surface, and q_{ref} was estimated from the measured dew point temperature at the leeward side of the wind tunnel. The reference wind speed U_{ref} was measured at a height of 20L. We repeated the same process at least three times for each array and used the averaged values of C_E in the following analysis.

The salinity change during the duration (2 h) was approximately 2×10^{-4} kg/kg for all the arrays, which indicated that the experimental error due to the salinometer was within 1% of the evaporation flux. The saltwater surface lowered about 0.4 mm, which was much smaller than the size of the blocks (25 mm); hence, the change of geometry due to evaporation can be considered negligible.

The Reynolds number (Re) based on the dimension of the blocks and the wind speed at 20L was about 3300, and the roughness Reynolds number ($Re*$) based on friction velocity and roughness length was about 60. According to Snyder and Castro (2002), a boundary layer over a fully rough surface, where the effect of viscosity is negligible, is observed if the roughness Reynolds number Re_* based on the roughness length and friction velocity, exceeds O (1); hence, Re_* for our experiment satisfied the criteria for a fully rough surface similar to an actual urban surface.

3 EXPERIMENTAL RESULTS

The relation between the estimated values of C_E and λ_p is shown in Figure 3. The result for a smooth surface with no obstacle is shown as a reference. In addition, the drag coefficients C_d measured by Hagishima et al. (2009) are also plotted for arrays with the same configuration as our present research. The definition of C_d is as follows:

$$C_d = \frac{\tau_0}{0.5\rho_{air}U_{ref}^2}$$
(6)

where τ_0 is total surface shear stress of an urban area (Pa). The reference mean flow speed for both C_E and C_d was that measured at a height of 20L.

The effect of a block array on the scalar transfer of the street surface is affected by the following two different mechanisms: (1) since a block array decreases the mean flow near the street surface, it will decelerate the scalar exchange between the surface and air due to advection, and (2) in contrast, 3-D vortices around blocks will effectively make the sublayer near the street surface thinner and will enhance vertical turbulent mixing; hence a block array will work to increase C_E for the street surface. The fact that all the values of C_E for ST1 and SQ1 were larger than that for the smooth surface indicates that the latter effect prevailed here.

When we compared the tendencies of the staggered and square arrays, C_E of the cubical staggered array (ST1) against λ_p showed a peak at $\lambda_p = 17.4\%$. In contrast, C_E of the square array (SQ1) decreased monotonically with the increase of λ_p. In addition, the values of SQ1 and ST1 were almost the same under the condition of $\lambda_p = 7.7\%$ and that of ST1 was larger than that of SQ1 under the higher λ_p condition. Such a tendency is probably related to the

flow characteristics of each array. It is well known that canopy flow can be classified into three regimes according to the roughness packing density, namely, isolated flow for sparse canopy, wake interference flow for a medium roughness density condition, and skimming flow for dense canopy (Oke, 1988).

The agreement of C_E for the $\lambda_p = 7.7\%$ condition might have been due to an isolated flow regime (note that this condition is lower than the value of λ_p for the C_d peak). In other words, the layout of the blocks did not affect the scalar transfer of the street surface because the interference of airflow around each block was weak. In contrast, in the staggered array, scalar transfer of the street increased with λ_p under the condition of λ_p from 7.7% to 17.4%. Considering the tendency of C_d, the flow regime of this condition was either an isolated flow or a wake interference flow. Hence, an increase in λ_p indicates an increase in the number of obstacles in the salt water surface; these obstacles generate 3-D airflow near the street surface, which enhances the vertical mixing. Such behavior might have resulted in the increase of C_E against λ_p. The decrease of C_E for large λ_p conditions was probably caused by both the decreased advection effect due to low wind speed near the surface, and weakened vertical mixing due to a skimming flow regime.

C_E of the staggered array was larger than that of the square array under the condition of $\lambda_p > 17.7\%$. This may have been caused by the fact that the 3-D airflow consisted of various sizes of vortices around the blocks (Coceal et al., 2006, 2007), which enhanced the introduction of dry air near the street surface. Since the distance between the blocks of the staggered array in the mean wind direction was greater than that of the square array, the leeward area of the blocks affected by the vortices of the staggered array was greater than that of the square array.

4 CONCLUSIONS

We used the so-called salinity method to estimate the scalar transfer rate from the floor surface of a block array in a wind tunnel. We calculated the estimated transfer coefficients for cubical arrays with staggered and square layouts under different conditions of roughness packing density. Our results reveal that a block array enhances the vertical mixing and increases the transfer coefficient of the street surface. In addition, the transfer coefficient of the street surface of a staggered array is larger than that of a square array under skimming flow or wake interference flow.

References

Barlow J.F., Harman I.N., Belcher S.E 2004. Scalar Fluxes from urban street canyons, Part 1: Laboratory simulation. Boundary-Layer Meteorology 113, 369–385.

Brutsaert W. 1982. Evaporation into the atmosphere. D. Reidel Publishing Company, Dordrecht, The Netherlands.

Chamberlain A.C. 1968. Transport of gases to and from surfaces with bluff and wave-like roughness elements. Quarterly Journal of the Royal Meteorological Society 94(401), 318–332.

Cheng H, Castro I.P. 2002. Near wall flow over urban-like roughness. Boundary-Layer Meteorology 104:229–259.

Chyu M.K. and Goldstein R.J. 1986. Local Mass Transfer in Rectangular Cavities with Separated Turbulent Flow. Eighth International Heat Transfer Conference 3, 1065–1070.

Coceal O., Thomas T.G., Castro I.P., Belcher S.E. 2006. Mean flow and turbulence statistics over groups of urban-like cubical obstacles. Boundary-Layer Meteorology 121, 491–519.

Coceal O., Thomas T.G., Belcher S.E. 2007. Spatial variability of flow statistics within regular building arrays. Boundary-Layer Meteorology 125, 537–552.

Grimmond C.S.B., Oke T.R. 1999. Aerodynamic properties of urban areas derived from analysis of surface form. Journal of Applied Meteorology 38, 1262–1292.

Hagishima A., Tanimoto J., Narita K-I. 2005. Intercomparisons of experimental convective heat transfer coefficients and mass transfer coefficients of urban surfaces. Boundary-Layer Meteorology 117, 551-576.

Hagishima A., Tanimoto J., Nagayama K., Meno S. 2009. Aerodynamic parameters of regular arrays of rectangular blocks with various geometries. Boundary-Layer Meteorology 132, 315–337.

Kanda M. 2006. Large-eddy simulations on the effects of surface geometry of building arrays on turbulent organized structures. Boundary-Layer Meteorology 118, 151–168.

Kanda M., Moriizumi T. 2009. Momentum and heat transfer over urban-like surfaces. Boundary-Layer Meteorology 131, 385–401.

Narita L-K-I. 2007. Experimental study of the transfer velocity for urban surfaces with a water evaporation method. Boundary-Layer Meteorology 122, 293-320.

Oke T.R. 1988. Street design and urban canopy layer climate. Energy and Buildings 11, 103–113.

Owen P.R., Thomson W.R. 1963. Heat transfer across rough surfaces. Journal of Fluid Mechanics 15(3), 321–334.

Pascheke F., Barlow J.F., Robins A. 2008. Wind-tunnel modelling of dispersion from a scalar area source in urban-like roughness. Boundary-Layer Meteorology 126, 103-124.

Snyder W.H., Castro I.P. 2002. The critical Reynolds number for rough-wall boundary layers. Journal of Wind Engineering and Industrial Aerodynamics 90, 41–54.

(a) SQ1   (b) ST1
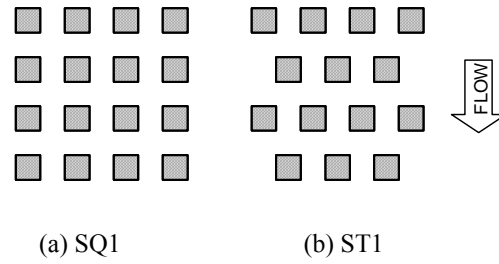
Figure 1. Schematic plan views of regular arrays used for the experiment.
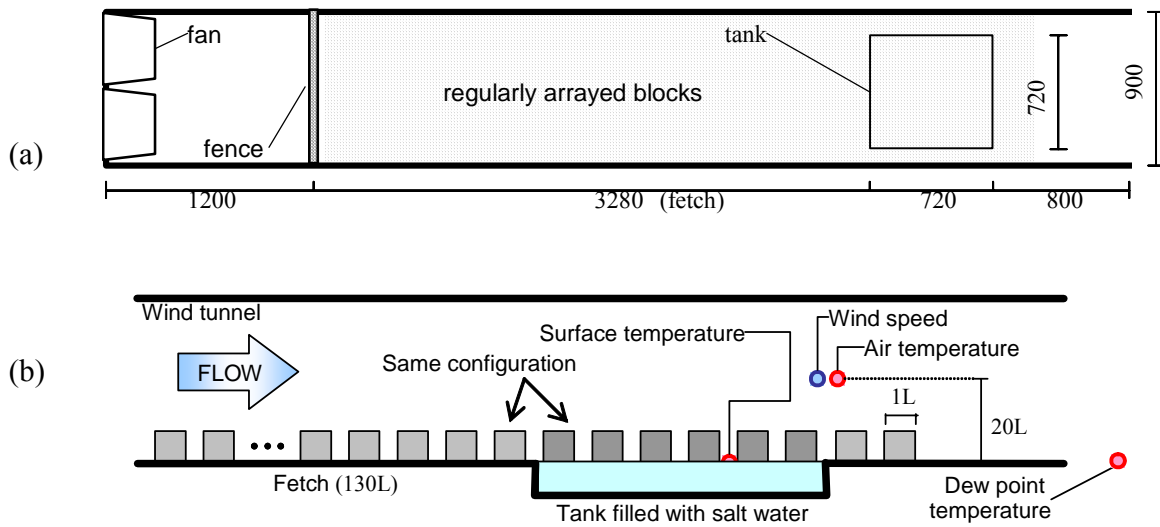
Figure 2. Wind tunnel device. (a) Schematic plan view [in mm], (b) diagrammatic elevation view.
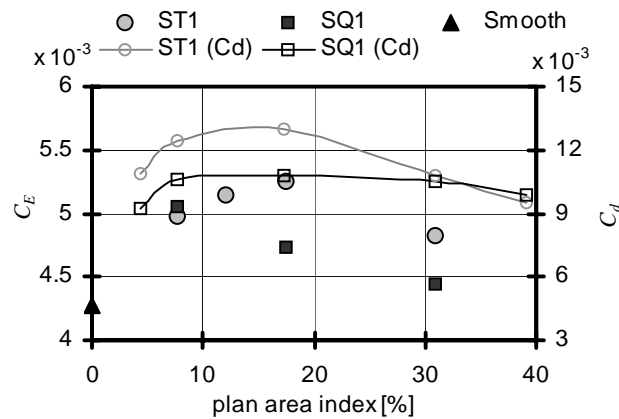
Figure 3. Transfer coefficient C_E of cubical arrays under various conditions of plan area index (λ_p). ST1 (C_d) and SQ1 (C_d) denote the drag coefficients of cubical staggered and square arrays measured by Hagishima et al. (2009).